Cell competition regulates the kinetics of thymopoiesis and thymus cellularity

Camila V. Ramos[1], Luna Ballesteros-Arias[1], Joana G. Silva[1], Marta Nogueira[1], Erida Gjini[2], Vera C. Martins[1, 3]

[1]Lymphocyte Development and Leukemogenesis Laboratory, Instituto Gulbenkian de Ciência, Calouste Gulbenkian Foundation, Oeiras, 2780-156, Portugal

[2]Mathematical Modeling of Biological Processes Laboratory, Instituto Gulbenkian de Ciência, Calouste Gulbenkian Foundation, Oeiras, 2780-156, Portugal

[3] Corresponding author: Vera C. Martins (email: vmartins@igc.gulbenkian.pt)

ORCID: 0000-0001-8717-9709

SUMMARY

Cell competition in the thymus is a homeostatic process that drives cellular turnover. If the process is impaired, thymopoiesis can be autonomously maintained for several weeks, but such condition is permissive to leukemia. We aimed to understand the impact of cell competition on thymopoiesis, identify the cells involved and determine how the process is regulated. Using thymus transplantation experiments we found that cell competition is mediated by double negative 2b (DN2b) and 3 (DN3) thymocytes and inhibits thymus autonomy. The expansion of the DN2b is regulated by a negative feedback loop imposed by double positive thymocytes and determines the kinetics of thymopoiesis. This feedback loop impacts on cell cycle duration of DN2b, in a response controlled by interleukin 7 availability. Altogether, we show that thymocytes do not merely follow a pre-determined path if provided with the correct signals. Instead, thymopoiesis results from the dynamic integration of cell autonomous and non-cell autonomous aspects that fine-tune normal thymus function.

KEYWORDS

T cell development, T lymphocyte differentiation, thymus, thymopoiesis, Cell competition, interleukin 7

INTRODUCTION

The thymus is an organ with high cellular turnover in which virtually all thymocytes are replaced every four weeks (Berzins et al., 1998). Progenitors of bone marrow origin enter the thymus at the cortico-medullary junction, commit to the T cell lineage, and progressively go through a series of differentiation stages before becoming T lymphocytes (Yui and Rothenberg, 2014). Each differentiation stage is brief and thymocytes at each stage are constantly replaced by new incoming cells (Petrie and Zuniga-Pflucker, 2007). The process of T lymphocyte differentiation is associated with thymocyte migration from the cortico-medullary junction through the cortex towards the sub-capsular zone, then back through the cortex, and finally into the medulla (Lind et al., 2001; Porritt et al., 2003). Migration in the thymus is regulated and reflects the existence of several niches, each supplying specific signals that are required for the stage-specific differentiation of thymocytes (Petrie and Zuniga-Pflucker, 2007; Takahama et al., 2017).

Normal thymopoiesis relies on the continuous seeding of the thymus by uncommitted progenitors of bone marrow origin (Love and Bhandoola, 2011; Rothenberg, 2019). Notwithstanding, thymus transplantation experiments revealed that if deprived of *de novo* progenitor seeding, the thymus is capable of maintaining T lymphocyte production independently of bone marrow contribution for several weeks (Martins et al., 2012; Peaudecerf et al., 2012). This condition is termed thymus autonomy. In the steady state, thymus autonomy is actively inhibited by cell competition. Specifically, thymocytes at the same differentiation stage but with shorter time of thymus residency outcompete and replace those with longer dwell time in the thymus, thereby promoting turnover (Martins et al., 2014). Failure in cell competition can be achieved experimentally in thymi grafted into recipients that either lack progenitors capable of thymic colonization, or that are deficient for interleukin 7 receptor (IL-7r) (Ballesteros-Arias et al., 2019; Martins et al., 2014). In either condition, the thymus grafts have a period of thymus autonomy that is then followed by T cell acute

lymphoblastic leukemia (T-ALL) with onset at 15 weeks post transplantation and incidence reaching up to 80% (Ballesteros-Arias et al., 2019; Martins et al., 2014). Such results illustrate the importance of cell competition in the maintenance of thymus homeostasis.

Cell competition was originally described in *Drosophila* (Morata and Ripoll, 1975) as a cellular interaction contributing to tissue homeostasis and optimal organ function (Baker, 2017; Johnston, 2009; Morata and Ballesteros-Arias, 2014; Moreno, 2008). It considers that if there is heterogeneity in fitness within a tissue, cells are capable of sensing that some clones are less fit than others. Those less fit, the losers, are eliminated as the result of intercellular interactions, while the more fit, the winners, prevail and contribute in full to the tissue. Of note, loser cells are viable and capable of maintaining tissue function. Their elimination results from the presence of winners in close proximity in the same tissue. Cell competition has been extensively studied in *Drosophila* and several studies in rats and mice have validated this as an important process in mammals (Claveria and Torres, 2016; Di Gregorio et al., 2016; Maruyama and Fujita, 2017). In the hematopoietic system, cell competition was found to be important for maintaining a fit population of hematopoietic stem cells following stress induced by mild irradiation (Bondar and Medzhitov, 2010). While it is clear that cell competition is an important homeostatic process, there is evidence that several molecular mechanisms are involved, that depend on the cellular context (Claveria and Torres, 2016; Maruyama and Fujita, 2017).

Here we sought to address the conditions that regulate thymus turnover and study how thymocyte subpopulations maintain stable thymopoiesis. Using thymus transplantation experiments we show that cell competition takes place in the thymic cortex, involves the double negative 2b (DN2b) and 3 (DN3) thymocytes and results in the inhibition of thymus autonomy. The expansion of the DN2b is regulated by a negative feedback loop imposed by double positive thymocytes, thereby defining the

kinetics of thymus turnover. We show that DN2b transiently adjusted their absolute cell numbers to the time requirement for the differentiation of double positive thymocytes. This impacted progressively on the absolute cell number of the following differentiation stages, slowing down thymopoiesis, when double positive thymocytes remained longer at that stage. Specifically, DN2b proliferated less when double positive thymocytes overexpressed a *Bcl2* transgene, as compared to when double positive thymocytes were non-transgenic. The rate of proliferation of the DN2b did not depend directly on the number of cells entering cell division, but instead on the duration of cell cycle in a process that was regulated by IL-7 availability. By comparing thymopoiesis between identical hosts, and changing the genotype of thymus donors, we could determine that thymocytes do not merely follow a pre-determined path if provided with the correct signals. Instead, thymopoiesis results from the integration of cell autonomous and non-cell autonomous aspects, both contributing to the kinetics of differentiation of T lymphocytes.

RESULTS

Thymus turnover is regulated by cell competition in double negative thymocytes

Thymopoiesis is regulated by several factors, and many of the genetic and molecular players regulating T lymphocyte differentiation are well-known (Rothenberg, 2019). These include factors expressed by thymocytes themselves, factors expressed by the thymic stroma, and the result of the interaction between thymocytes and stroma (Takahama et al., 2017). Steady state thymopoiesis relies on the constant replenishment of thymocytes by fit bone marrow derived progenitors (Boehm, 2012). In the absence of constant replenishment, the thymus is capable of autonomously maintaining T lymphocyte production but T-ALL emerges as a consequence (Ballesteros-Arias et al., 2019; Martins et al., 2014). To identify the cell populations that are involved in cell competition in the thymus, we grafted newborn thymi under the kidney capsule of adult recipients. Donor and host derived cells were distinguished based on the differential expression of CD45.1 and CD45.2 (Fig. 1A). The use of thymus transplants is advantageous because it allows assessment of the dynamics of thymopoiesis, while distinguishing cells with different dwell time in the thymus that are at the same stage of differentiation. As expected, when wild type thymus grafts were transplanted into wild type hosts, virtually all thymocytes were replaced after 4 to 5 weeks (Fig. 1B). The most immature populations of thymocytes, i.e. early T lineage progenitors (ETP) and double negative (DN) 2a, that were present in the thymus donors at the time of transplantation, differentiated and by seven days after transplantation no cells of thymus donor origin could be detected at those stages (Fig. 1C). One week later, by 14 days post-transplantation, ETP and DN2a populations were completely composed of host derived cells, indicating that the differentiation of these populations progresses normally upon transplantation (Fig. 1C). This observation was consistent in all conditions tested, regardless of the genotype of the donors and of the hosts (data not shown), which suggests that ETP and DN2a are not involved in cell competition and depend solely from thymus seeding. From the DN2b stage of differentiation onwards, we could observe that donor and host derived thymocytes coexisted, and

detail the kinetics with which host derived cells progressively replaced the donor derived thymocytes (Fig. 1D). To define the spatial localization of thymocytes, we performed immunohistological analyses of thymus grafts at various time points after thymus transplant (Fig. 1E). CD25 expression enabled the detection of DN2 and DN3 cells, and the co-staining with CD45.2 discriminated between donor and host thymocytes (Fig. 1E). Cortical and medullary areas could be easily distinguished by cytokeratin 8 (K8) staining that labels cortical thymic epithelial cells (Fig. 1E). This separation was also confirmed by nuclear counterstaining for Dapi, which shows cortical areas that are denser than the medullary areas (not shown). Overall, thymocytes followed the normal, well-known migratory trajectory throughout the thymus (Fig.1E). Specifically, CD25-positive thymocytes, i.e. DN2 and DN3, were dispersed in the cortex and accumulated at the sub-capsular zone (Fig. 1E). Overall results for the kinetics of turnover were similar to those obtained by flow cytometry (Fig. 1F). The quantification of the thymus sections showed that at stages when both donor and host derived CD25-positive thymocytes could be detected, their spatial distribution was consistent with the migration of donor derived cells, with longer time of thymus residency, 'ahead' of the host derived cells. Hence, host derived thymocytes were detected at the sub-capsular zone at later time-points of analysis (Fig. 1G). Altogether, these data show that donor- and host-derived thymocytes coexist in time starting at DN2b, but not earlier stages. The assumption that cell competition is an intra-stage specific interaction therefore suggests that ETP and DN2a subsets are unlikely to be involved. Furthermore, the histological data show that donor and host DN2b and DN3 can locate to the same regions of the thymus. Since donor and host cells in this experimental setting represent cells with different dwell times in the thymus, it is conceivable that they interact directly, and that such interaction controls the inhibition of autonomy.

Classical thymus transplantation experiments into immunodeficient hosts never demonstrated thymus autonomy because the host hematopoietic progenitors could colonize the thymus grafts and initiate

thymopoiesis (Frey et al., 1992; Takeda et al., 1996). We reasoned that such experimental setting could be informative about the thymocyte populations involved in cell competition and how they impact on thymopoiesis. To address those points, we grafted wild type donor thymi under the kidney capsule of *Rag2*$^{-/-}$ recipients (Fig.2A). *Rag2*$^{-/-}$ thymocytes cannot rearrange their T cell receptor *loci* and therefore fail to differentiate beyond the DN3e stage. Similar to the previous experiments, we never detected coexistence of donor and host thymocytes at the ETP and DN2a stages (not shown). On the other hand, DN2b and DN3 thymocytes were detected in coexistence at various time-points after transplantation, and the differentiation and emigration of wild type T lymphocytes from the thymus grafts in *Rag*-deficient recipients occurred with kinetics that were similar to those observed in wild type hosts (Fig. 1D, 2B). The only difference was that thymopoiesis in *Rag2*$^{-/-}$ recipients ceased after one single wave of donor T lymphocyte production, as expected, since *Rag*-deficient thymocytes are developmentally arrested at the DN3 stage. The fact that the analyzed wave of thymopoiesis was similar in wild type and in *Rag2*$^{-/-}$ recipients suggests that T lymphocyte differentiation is mostly regulated in a cell autonomous way from the DN3 stage onwards. Cell competition occurs between thymocytes at the DN2b and DN3 stages of differentiation, i.e. younger DN2b and DN3 thymocytes of host origin replace the "older" DN2b and DN3 thymocytes of donor origin that would otherwise be able to persist in an autonomous state. This interaction inhibits thymus autonomy and requires only the presence of young DN2b to DN3 but no other differentiation stages.

Wild type DN2b and DN3 thymocytes adjust cell numbers transiently according to feedback from more mature developmental stages

Thymopoiesis is generally considered from the perspective that developing thymocytes follow a rather complex but predefined program. In this context, if provided with the correct signals from the thymic stroma, thymocytes either progress and differentiate, or die. The prediction from this view is that thymopoiesis will depend exclusively on an intrinsic program in the thymocytes and will steadily

differentiate. In the same line, the kinetics of thymus turnover is also expected to remain constant. We sought to test if that was indeed the case, or whether thymocytes were capable of integrating information derived from the differentiation of more mature stages. To that end, we selected *Bcl2* transgenic mice that overexpress a human *BCL2* transgene in the T lymphocyte lineage (Katsumata et al., 1992; Strasser et al., 1991). *BCL2* overexpression delays apoptosis in thymocytes, mostly during positive selection (Akashi et al., 1997; Kondo et al., 1997), and we predicted that the kinetics of thymus turnover would be prolonged in time. Nevertheless, *Bcl2* transgenic thymi are very similar to thymi of wild type littermates in terms of the composition of thymocyte subpopulations (Supplemental Fig. 1A). The expression of endogenous *Bcl2* is unaltered in the transgenic thymi (Supplemental Fig. 1B), and only the transgene is responsible for an increased expression of BCL2 in thymocytes (Supplemental Fig. 1C). This does not grossly affect thymus cellularity, although we could detect that the total number of ETP and CD8 single positive cells was mildly increased (Supplemental Fig. 1D). The total number of DN2b and DN3 were both reduced when compared to wild type littermates (Supplemental Fig. 1D). No statistically significant differences were detected in the percentage of Annexin V-positive cells in *Bcl2* transgenic thymocytes as compared to wild type littermates (Supplemental Fig. 1E). Instead, we detected a reduction in the percentage of proliferating *Bcl2* transgenic thymocytes (Supplemental Fig. 1F), in accordance with previous reports (Mazel et al., 1996; O'Reilly et al., 1997).

To find out whether thymocyte subpopulations could detect and react to changes in the speed of differentiation of more mature populations, we compared thymus turnover in wild type versus *Bcl2* transgenic donor thymi following transplantation into wild type recipients (Fig. 3A). In this experimental setting, recipient derived thymocytes were always wild type and the difference was in the genotype of the donor thymus (Fig. 3A). The prediction was that if the kinetics of thymus seeding and early thymopoiesis would rely solely on the wild type genotype of the incoming cells, then host

derived thymocytes would seed the thymus graft and differentiate identically in both conditions. Instead, we observed that when wild type thymocytes differentiated in a *Bcl2* transgenic thymus, they did so with a delayed kinetic as compared to that of wild type thymocytes in a wild type thymus graft (Fig. 3B, C). Depicted are (representative) examples of thymocytes from grafts 21 days post-transplant, in which the differentiation of wild type host derived thymocytes is delayed in the *Bcl2* transgenic thymus as compared to thymocytes differentiating in the wild type thymus (Fig. 3 B). This delay in thymocyte replacement was most obvious for double positive thymocytes, for which the curves describing donor and host derived cells cross each other at day 17 in the wild type, or 21 in the *Bcl2* transgenic grafts (Fig. 3C). Nevertheless, measuring thymocyte populations only by percentages could be misleading, as they could reflect the accumulation of the *Bcl2* transgenic donor rather than a difference in host derived thymocytes. Therefore, we quantified the absolute number of cells within each compartment over time and detected that wild type thymocytes of host origin were indeed transiently reduced in numbers at the DN2b and DN3 stages specifically in *Bcl2* transgenic thymus, as compared to their counterparts differentiating in wild type thymus donors (Fig. 3D). The delay in the expansion of host derived DN2b and DN3 thymocytes correlated with the time required for double positive *Bcl2* transgenic donor cells to progress out of this developmental stage (Fig. 3D), consistent with the rescue from failed positive selection induced by the transgene (Strasser et al., 1991). This difference disappeared at later time-points, in accordance to the time required for donor thymocytes to differentiate (data not shown). The fact that the numbers of DN2b and DN3 wild type thymocytes were transiently reduced in the *Bcl2* transgenic thymus as compared to the numbers in the wild type thymus suggests that thymocytes can detect and respond to differences in the thymus graft, with consequences on the total time of thymus turnover. Specifically, the time required for more mature thymocytes, presumably the double positive, to differentiate was determining in the expansion rate and differentiation capacity of DN2b and DN3.

Bcl2 transgenic DN2b and DN3 thymocytes adjust cell numbers transiently according to feedback from more mature developmental stages

We reasoned that if DN2b and DN3 adjusted cell numbers according to more differentiated thymocytes this was likely to be a general property and should not be restricted to wild type thymocytes. Therefore, we tested whether *Bcl2* transgenic thymocyte subpopulations could also react to changes in the speed of differentiation of more mature populations, and whether that influenced thymus turnover. For that purpose, we compared thymus turnover in wild type versus *Bcl2* transgenic donor thymus upon transplantation into *Bcl2* transgenic recipients (Fig. 4A). Much in line with the former results (Fig. 3), we observed that the kinetics of turnover of *Bcl2* transgenic thymocytes differentiating in a *Bcl2* transgenic thymus, was delayed as compared to those differentiating in a wild type thymus graft (Fig. 4B, C). This was confirmed by quantification of the absolute number of thymocytes within each compartment over time (Fig. 4D). Host derived thymocytes at the DN2b and DN3 stages were transiently reduced in numbers in the *Bcl2* transgenic thymus (Fig. 4D). The fact that *Bcl2* transgenic thymocyte numbers at the DN2b and DN3 were transiently reduced in the *Bcl2* transgenic thymus as compared to the numbers in the wild type thymus is consistent with the results obtained for wild type host derived thymocytes. Altogether, our results show that DN2b and DN3 adjust their numbers transiently, according to the speed of differentiation of more differentiated thymocytes. This is a general property that does not depend on the genotype of the recipient bone marrow derived cells, but instead reflects their response to the environment that they encounter in the thymus (Fig. 3, 4).

In addition to the adjustment in cell numbers that occurred at DN2b and DN3stages, we also detected that host derived ETPs were increased in the wild type thymus grafts as compared to the same population in *Bcl2* transgenic thymus grafts. This was the case both in wild type (Fig. 3D) and *Bcl2* transgenic recipients (Fig. 4D). Changes in the number of ETP could be explained either by

differences in thymus seeding by bone marrow derived progenitors, or by differential expansion of the population of thymus seeding progenitors in the wild type thymus versus the transgenic thymus. We consider the latter explanation more likely, as the hosts are identical and only the thymus grafts differ.

DN2b control cellularity by adjusting cell cycle duration, thereby determining the kinetics of thymus turnover

The observed differences in the absolute number of DN2b and DN3 could result from either differential cell death or proliferation rates. We measured apoptosis by Annexin V staining and detected a reduction in the percentage of Annexin V positive DN2 and DN3 wild type thymocytes in the *Bcl2* transgenic thymus grafts as compared to the same subsets differentiating in the wild type grafts (Fig. 5A). Next we assessed proliferation by *in vivo* EdU incorporation following a 2-hour pulse. By 14 days after transplantation, host derived wild type DN2 thymocytes differentiating in *Bcl2* transgenic thymus grafts had a lower percentage of EdU-positive cells than DN2 differentiating in wild type thymus grafts (Fig. 5B). This difference was transient, as two days later the rate of proliferation at the DN2 increased and even surpassed that of cells differentiating in wild type thymi (Fig. 5B). The transient reduction in the percentage of EdU-positive cells could result from a reduced number of cells effectively entering cell cycle, or from a reduction in the duration of cell cycle. To address this point, we performed an EdU/BrdU double pulse assay (Fig. 5C) to identify cells that labelled with either one, with both, or neither of the DNA intercalating agents (Fig. 5D), as previously described (Akinduro et al., 2018). We used these data to develop a mathematical model that allows calculation of the duration of cell cycle and discriminating the contribution of S phase from G1/G2/M for the thymocyte populations of interest (Methods section). The model consists of a two-state system in which cells can either be in S phase or outside S phase (supplemental Fig. 2A). The population outside S phase is composed of actively cycling cells (that can be in G1, G2 or M) and cells arrested

in G0. The model generates four values (corresponding to the proportion of cells in each quadrant of the EdU/BrdU profile) as a function of the proportion of cycling cells, their respective cell cycle length, and the elapsed time between the two pulses. We validated the model by plotting generated and experimental values (supplemental Fig. 2B) prior to use it to determine cell cycle duration of wild type DN2 and DN3 early (DN3e – negative for intracellular TCRβ) thymocytes in either wild type or *Bcl2* transgenic thymus grafts (Fig. 5E). We could determine that both DN2 and DN3e prolonged cell cycle duration transiently in *Bcl2* transgenic thymi (Fig. 5E). Moreover, we show that although the duration of the whole cell cycle was affected, this was mostly due to an increase in the duration of the S phase (Fig. 5F), and not to differences in the duration of G1/G2/M (Supplemental Fig. 2C). Taken together, the data show that DN2b react differently to the thymus in which they differentiate mostly by altering the duration of cell cycle, and not by changing the proportion of cells that effectively enter cell cycle (Fig. 5G).

The changes in proliferation and numbers of DN2b and DN3 depend directly on the presence of double positive thymocytes

The data so far is consistent with the idea that the transient response of the DN2b – slowing down cell cycle, with the resulting impact on cell numbers, thereby prolonging the kinetics of thymus turnover in the *Bcl2* transgenic thymus – is caused by the longer endurance of thymocytes at the double positive stage. If that were indeed the case, then that response should be absent in a *Rag*-deficient background, which lacks double positive thymocytes. It is reasonable to consider that double negative and double positive thymocytes could interfere with each other, since they both locate in the thymic cortex. There, they might either compete directly for common resources, or the much larger double positive population could interfere with the normal migration pattern of the DN2b thymocytes, and the way the latter reach the niches that enable differentiation. To test this, we performed thymus transplantation experiments similar to those depicted in Figure 3 but in *Rag*-deficient (*Rag2*$^{-/-}$)

background (Fig. 6A). *Rag2*$^{-/-}$ thymocytes fail to differentiate beyond the DN3e stage, because they cannot rearrange the T cell receptor *loci*, so double positive thymocytes are never generated. The hematopoietic progenitors seeding the thymus grafts were *Rag2*$^{-/-}$ and they seeded a *Rag2*$^{-/-}$ thymus that was either *Bcl2* transgenic, or non-transgenic (Fig. 6A). In this experimental setting, thymopoiesis up to the DN3 stage progressed in both conditions (Fig. 6B). We observed that the cell numbers of host derived DN2b and DN3 in *Bcl*2 transgenic or non-transgenic thymus grafts no longer differed significantly in the *Rag*-deficient background (Fig. 6C). This indicates that double positive thymocytes interfere with the pace of differentiation of the more immature thymocytes. Furthermore, no difference was detected in the percentage of proliferating DN2b and DN3 thymocytes (Fig. 6D). The fact that the cell numbers of host derived DN2b and DN3 thymocytes were the same in *Rag2*$^{-/-}$ *Bcl*2 transgenic and *Rag2*$^{-/-}$ non-transgenic thymus grafts suggests that double positive thymocytes influence the expansion of DN2b. The result of that interaction is determining for the pace of differentiation at the double negative stages, which in turn defines overall thymus turnover.

The changes in proliferation and numbers of DN2b and DN3 are regulated by IL-7 availability

IL-7/IL-7r signaling is important for proliferation and survival of thymocytes at the DN2 stage, and leads to their differentiation into DN3 thymocytes (DiSanto et al., 1995; Peschon et al., 1994; von Freeden-Jeffry et al., 1995). Since IL-7 is limiting in the thymus (Barata et al., 2019), we reasoned that IL-7 availability could regulate proliferation, thereby controlling absolute cell numbers of DN2b and DN3 thymocytes. To test that hypothesis, we took advantage of IL-7r heterozygote (*IL-7rα*$^{+/-}$) mice, that have normal thymopoiesis (Supplemental Fig. 3A) but express less surface IL-7r (Supplemental Fig. 3B). Since the levels of available IL-7 are controlled by cellular intake (Martin et al., 2017), *IL-7rα*$^{+/-}$ thymi are predicted to have higher levels of IL-7. We transplanted *IL-7rα*$^{+/-}$ *Bcl2* transgenic versus *IL-7rα*$^{+/-}$ (non-transgenic) thymi into wild type recipients (Fig. 7A). In this experimental setting, recipient derived thymocytes were always wild type and seeded *IL-7rα*$^{+/-}$

thymus grafts, in which IL-7 was less limiting. If increased availability of IL-7 increases the differential proliferation of DN2b when differentiating in a *Bcl2* transgenic versus a non-transgenic thymus, then the prediction is that the differences detected previously (Fig. 3, 5) would subside. Indeed, the differences in cell numbers (Fig. 7B), percentage of proliferating cells (Fig.7C), duration of cell cycle (Fig.7D), and percentage of cells in cell cycle (Fig.7E) were all lost. Hence, IL-7 availability regulates the differential proliferation of DN2b that occurs in response to double positive thymocytes.

Taken together, our data show that thymocytes at the DN2b control the kinetics of thymus turnover, reacting to the speed at which more differentiated progeny progresses in thymopoiesis. DN2b thymocytes impact on thymus turnover by adjusting cell cycle duration in an IL-7rα dependent way, which directly affects absolute cell numbers within the DN2b. This propagates onto the numbers of DN3 and then s subsequently onto the following stages of differentiation.

DISCUSSION

Previous work has demonstrated that cell competition between thymocytes promotes thymus cellular turnover and is required to prevent thymus autonomy and T-ALL (Martins et al., 2014). Impaired cell competition results from a setting in which the thymus is deprived of *de novo* seeding by hematopoietic progenitors, or if the progenitors colonizing a wild type thymus lack IL-7r (Martins et al., 2014). In either case, thymus autonomy is triggered and maintained for some time (Martins et al., 2012; Peaudecerf et al., 2012). Our previous work showed that all conditions in which thymus autonomy was detected, the long term consequence was the emergence of T-ALL (Ballesteros-Arias et al., 2019). Here we show that cell competition takes place in the thymic cortex, identify the cell populations involved, and their expansion is regulated by a feedback loop mechanism imposed by more mature thymocytes. Cell competition involves DN2b and DN3 thymocytes and inhibits thymus autonomy. Donor and host cells at the same differentiation stages have effectively different dwell time in the thymus, i.e. donor cells reside in the thymus grafts for longer time than the host counterparts. The presence of the host DN2b to DN3 was necessary and sufficient to inhibit the persistence of donor thymocytes that would have the potential to maintain thymus autonomy, and later generate T-ALL. It remains to be seen if this interaction involves direct cell-cell contacts, but the presence of thymocytes with different dwell time in the same regions of the thymus is consistent with that hypothesis. There is a step of regulation of DN2b thymocyte expansion that is imposed by double positive thymocytes. This second interaction results in the control of proliferation, and thereby differentiation, of the more immature cells. As a consequence, the effective expansion of the population, and consequently the absolute cell numbers of DN2b are defined according to the time required for the differentiation of double positive thymocytes. Changes in cellularity of DN2b propagate sequentially, meaning that DN2b are effectively the cells defining the pace at which thymopoiesis proceeds, and thereby the kinetics of thymus turnover. It will be of interest to determine

whether this interaction results from competition for limiting resources or whether there is a limit imposed by availability of space in the cortex.

Competition for limiting resources, including cytokines, growth factors or available niches play a central role in the regulation of the immune system and in the maintenance of homeostasis in the steady state (Surh and Sprent, 2008). In the thymus, competition for stromal niches occurs at early stages of differentiation and defines the number of available niches that can be occupied by thymus seeding progenitors at any given time (Prockop and Petrie, 2004). What thymocytes compete for is still elusive, but limiting factors like Notch ligands and interleukin 7 (IL-7) are likely important. In this context, *Notch1*$^{+/-}$ progenitors generate reduced thymocyte progeny in mixed bone marrow chimeras, suggestive that Notch ligands are likely limiting, and potentially drive competition in the thymus (Tan et al., 2005). This is consistent with the competitive advantage of thymocytes overexpressing a Lunatic Fringe transgene, which confers cells with increased sensitivity to Notch1 (Visan et al., 2006). While the step at which cell competition takes place could be explained by the presence of new incoming cells, that respond to IL-7 and therefore displace those cells of donor origin, this effect cannot be explained by differential expression of IL-7r (not shown). It will be necessary to further detail the mechanism regulating this interaction. As for the negative feedback loop controlling DN2b expansion by double positive thymocytes, it is unlikely that DN2b and double positive thymocytes compete directly for access to the same ligands, as their requirements for differentiation do not seem to overlap (Yui and Rothenberg, 2014). Instead, we consider likely that the longer differentiation time of double positive *Bcl2* transgenic thymocytes translates into longer time of residence in the cortex, and that might interfere with the access of the proportionally very few DN2b to the ligands expressed by the thymic stroma. Indeed, there is on average a relation of 5000 double positive thymocytes for every DN2b, and the longer residence of double positive thymocytes could interfere with the migration of cells throughout the cortex. The fact that IL-7 availability regulates

expansion of DN2b under these conditions is not completely unexpected, as DN2b depend specifically on this cytokine to proliferate and differentiate (Cao et al., 1995; DiSanto et al., 1995; Peschon et al., 1994).

Further studies will additionally focus on understanding the factors enabling thymus autonomy, and how autonomy permits leukemia initiation (Paiva et al., 2018). In this context, it is interesting that the work from two independent groups using bone marrow chimeras points out that lymphoid malignancies emerge in *common gamma c* (γ_c) deficient hosts reconstituted with wild type bone marrow cells in limiting dosages (Ginn et al., 2017; Schiroli et al., 2017). In such conditions, it is likely that the efficiency of thymus seeding is compromised, with interspersed periods that are refractory to thymus colonization, and thymus autonomy is established. We consider likely that any condition that enables thymus autonomy for a prolonged time period is permissive to the emergence of T-ALL (Paiva et al., 2018).

Finally, cell competition was originally described and studied as a homeostatic process contributing to tissue homogeneity and optimal organ function (Amoyel and Bach, 2014; Claveria and Torres, 2016). The process we describe in the thymus is reminiscent of this role, even though the molecular mechanisms involved are probably different, as they ought to be cell context dependent. Furthermore, cell competition has been shown to protect from cancer in the mouse intestine, by extrusion of transformed epithelial cells into the lumen (Kon et al., 2017). Nevertheless, cell competition has also been implicated in cancer by promoting an advantage to tumor cells as opposed to the cells in the normal tissue (Eichenlaub et al., 2016; Madan et al., 2019; Suijkerbuijk et al., 2016). It will be of interest to determine whether a similar process plays a role in the initiation and progression of T-ALL.

ACKNOWLEDGEMENTS

This work was supported by the Instituto Gulbenkian de Ciência (IGC) of the Calouste Gulbenkian Foundation, and by the Portuguese National Research Council (Fundação para a Ciência e Tecnologia [FCT], Grant PTDC/BIA-BID/30925/2017) (to VCM). CVR is a PhD student of the IGC Integrative Biology and Biomedicine (IBB) PhD Program and is supported by an individual PhD Fellowship of the Portuguese National Research Council, FCT ref. PD/BD/139190/2018. This work was developed with the support of the research infrastructure Congento LISBOA-01-0145-FEDER-022170, co-financed by FCT and Lisboa2020, under the PORTUGAL2020 agreement (European Regional Development Fund). We acknowledge J Howard, HJ Fehling, J Carneiro, G Morata, RS Paiva and RA Paiva for critical reading of the manuscript. We acknowledge V Correia for technical support. We thank the team of Animal House Facility of IGC for the outstanding support to this work, and acknowledge the Microscopy, Antibody, Histopathology and Flow Cytometry Units of IGC in supporting this work.

AUTHOR CONTRIBUTIONS

CV Ramos designed and performed experiments, analyzed data, developed the mathematical model to determine the duration of cell cycle and wrote the manuscript, L Ballesteros-Arias and JG Silva performed experiments and analyzed data, M Nogueira performed immunohistology, E Gjini contributed to the design and fit of the mathematical model to determine the duration of cell cycle, and VC Martins conceived the study, designed research, designed experiments, analyzed data and wrote the manuscript. All authors edited and contributed to the final version of the manuscript.

DECLARATION OF INTERESTS

The authors declare no competing interests.

FIGURE LEGENDS

Figure 1. Kinetics of thymus turnover in thymus transplants. (A) Schematics of the experimental design. Wild type (WT) newborn donor thymus lobes from an F1(B6xB6/Ly5.1) were transplanted under the kidney capsule of adult B6 wild type (WT) recipient mice. One thymus was grafted in each recipient. The exclusive expression of CD45.2 in host derived thymocytes enabled the distinction from donor derived thymocytes, that co-expressed CD45.1 and CD45.2 markers. **(B)** Thymocytes from thymus grafts were analyzed by flow cytometry at the indicated time points after transplant (in days, d) and the relative proportion of donor (black circles and line) and host (green circles and line) are depicted for total thymocytes. Every thymus graft is represented by a symmetric pair of (black and green) dots. **(C)** Representative contour plots of thymocytes analyzed at the indicated time points (in days) after thymus transplant. Depicted is the expression of CD117 and CD25 in donor (CD45.2+ CD45.1+) or host (CD45.2+) thymocytes pre-gated for the markers $CD4^{-}CD8^{-}Lineage^{-}$. Gated populations from top left to bottom right are ETP, DN2a, DN2b, and DN3 **(D)** Absolute number of DN2b (top), DN3 (middle) and CD4+CD8+ double positive (DP, bottom) were determined at the indicated time-points after thymus transplants (in days, d). Donor and host derived thymocytes are represented in black or green bars, respectively. Data are representative of a minimum of two independent experiments with at least 6 grafts for each time point. Data are median +95% confidence interval. **(E)** Thymus grafts were analyzed by immunohistology for the indicated surface markers, CD25 (red), CD45.2 (green) and cytokeratin 8 (K8, in blue). Depicted is one representative example analyzed 7 days (left) or 14 days (right) after transplant. Magnification of 20X, scale bars = 50μm. For the experiments analyzed by immunohistology, the experimental design followed that in panel (A) but donors were B6/Ly5.1 (CD45.1) to enable the clear distinction from host cells (CD45.2+). Asterisk indicates a CD25+ cell of host origin (CD25 positive CD45.2 positive, in yellow). **(F)** Quantification of the relative proportion of donor (black circles and line) and host (green circles and line) cells in CD25+ thymocytes from thymus sections at different time-points post-engraftment.

Each circle represents one thymus section. **(G)** Stacked density distribution of the distance of donor and host-derived CD25+ cells to the capsule (normalized by the maximum distance observed) at different time-points of analysis. Host CD25+ cell density distribution is depicted in green and Donor CD25+ cell density distribution in black. N is the number of grafts analyzed, and numbers correspond to the number of CD25 positive thymocytes of donor (black) or host (green) origin at the indicated time-points.

Figure 2. Kinetics of wild type thymopoiesis in *Rag2*$^{-/-}$ recipients. (A) Schematics of the experimental design. Wild type (WT) newborn donor thymus lobes from an F1(B6xB6/Ly5.1) were transplanted under the kidney capsule of adult *Rag2*$^{-/-}$ recipient mice. One thymus was grafted per recipient. **(B)** Thymocytes from thymus grafts were analyzed by flow cytometry at the indicated time points after transplant (in days, d) and the absolute number of DN2b (left), DN3 (middle) and double positive (DP, right) were determined at the indicated time-points after thymus transplants (in days, d). Donor and host derived thymocytes are represented in black or green bars, respectively. ND = not detectable. Shown is representative data from one out of two independent experiments. Data are median + 95% confidence interval and a minimum of 4 grafts per time-point are depicted.

Figure 3. Wild type thymocytes have a slower kinetics of thymus turnover when seeding a *Bcl2* transgenic thymus. (A) Schematics of the experimental design. Wild type (WT) or *Tg(Bcl2)* newborn donor thymus lobes from an F1(B6 *Tg(Bcl2)*xB6/Ly5.1) were transplanted under the kidney capsule of B6 wild type (WT) adult mice. One thymus was grafted in each recipient. **(B)** Representative FACS plots of CD4/CD8 profile of live thymocytes from thymus grafts 21 days after transplant. Top left: donor wild type thymocytes; bottom left: donor *Tg(Bcl2)* thymocytes; top right: host wild type thymocytes in wild type thymus graft; bottom right: host WT thymocytes in *Tg(Bcl2)* thymus graft. **(C)** Proportion of donor and host thymocytes in Lin^{-} double negative (DN, left column)

and CD4+CD8 double positive (DP, right column) during thymus turnover in wild type grafts (top row) and *Tg(Bcl2)* grafts (bottom row). **(D)** Absolute number of host derived wild type (green bars) and donor (wild type = black bars, *Tg(Bcl2)* = gray bars) thymocytes in different developmental compartments during thymus turnover. For each time-point, left bar-plots correspond to wild type grafts and right bar-plots correspond to *Tg(Bcl2)* grafts. (D) Wilcoxon signed-rank test. *p≤0.05, **p≤0.01, ***p≤0.001, **** p<0.0001. Data are representative of at least three independent experiments and a minimum of 6 grafts per time-point. Data are median + 95% confidence interval.

Figure 4. *Bcl2* transgenic thymocytes have slower kinetics of thymus turnover when seeding a *Bcl2* transgenic thymus. (A) Schematics of the experimental design. Wild type (WT) or *Tg(Bcl2)* newborn donor thymus lobes from an F1(B6 *Tg(Bcl2)*xB6/Ly5.1) were grafted under the kidney capsule of B6 *Tg(Bcl2)* adult mice. One thymus was grafted in each recipient. **(B)** Representative FACS plots of CD4/CD8 profile of live thymocytes from thymus grafts 14 days after transplant. Top left: donor wild type thymocytes; bottom left: donor *Tg(Bcl2)* thymocytes; top right: host *Tg(Bcl2)* thymocytes in donor wild type thymus; bottom right: host *Tg(Bcl2)* thymocytes in donor *Tg(Bcl2)* thymus. **(C)** Proportion of donor and *Tg(Bcl2)* host derived thymocytes in Lin^- double negative (DN, left column) and CD4+CD8 double positive (DP, right column) during thymus turnover in wild type grafts (top row) and *Tg(Bcl2)* grafts (bottom row). **(D)** Absolute number of *Tg(Bcl2)* host (blue bars) and donor (wild type = black bars, *Tg(Bcl2)* = gray bars) thymocytes in different developmental compartments during thymus turnover. For each time-point, left bar-plots correspond to wild type grafts and right bar-plots correspond to *Tg(Bcl2)* grafts. (D) Wilcoxon signed-rank test. *p≤0.05, **p≤0.01, ***p≤0.001, **** p<0.0001. Data are median+95% confidence interval and at least 4 grafts per time-point are depicted.

Figure 5. Delay in thymus turnover is associated to proliferation and cell cycle duration at the DN2b. (A) Experimental design followed the one depicted in Fig.3A and thymus grafts were analyzed by flow cytometry 14 days after transplantation. Graphs show percentage of Annexin V positive cells in DN2 and DN3e thymocytes. **(B)** Proliferation was determined in a 2-hour pulse EdU incorporation assay on days 14 and 16 after transplant, as indicated. Quantification of the percentage of EdU-positive thymocytes is depicted for the host derived, wild type DN2 and DN3e thymocytes. **(C)** Schematics of the experimental design for the experiments presented in panels (D) to (G). Newborn thymus donors with the indicated genotypes were transplanted under the kidney capsule of adult B6 wild type (WT) recipient mice, as in Fig.3. At 14 or 16 days after transplant, mice were injected intraperitoneally with EdU, followed by BrdU injection after a 2-hour interval. Thymus grafts were analyzed two hours later. **(D)** Representative dot plot of EdU/BrdU profile of host DN2 thymocytes 14 days after transplant. **(E)** Total cell cycle duration in hours (h), **(F)** duration of S phase, and **(G)** percentage of cycling cells in the indicated populations that differentiated in either non-transgenic (non-Tg) or in *Bcl2* transgenic, *Tg(Bcl2),* thymus grafts. Depicted are the results for day 14 (top panels) and day 16 (bottom panels) after transplant. Each dot corresponds to the estimate for one graft. Wilcoxon signed-rank test. *p≤0.05, **p ≤0.01, ***p≤0.001, **** p<0.0001. Data are representative of a minimum of two independent experiments. Points represent individual grafts, lines represent medians.

Figure 6. The changes in proliferation and numbers of DN2b and DN3 reflect the time requirement for differentiation of the double positive thymocytes. (A) Schematics of the experimental design. Newborn donor thymi of the indicated genotypes were transplanted under the kidney capsule of *Rag2*$^{-/-}$ adult mice. One thymus was grafted in each recipient. **(B)** Representative contour plots of CD117/CD25 profile of donor (left) and host derived (right) thymocytes in non-transgenic (top) or *Bcl2* transgenic (bottom) grafts 14 days after transplant. **(C)** Quantification of the

total number of host derived *Rag2*$^{-/-}$ (green bars) and donor derived (*Rag2*$^{-/-}$ = black bars, *Rag2*$^{-/-}$ *Tg(Bcl2)* = gray bars) thymocytes at ETP (left), DN2b (middle) and DN3 (right) stages of development during thymus turnover. For each time-point, left bar-plots correspond to *Rag2*$^{-/-}$ grafts and right bar-plots correspond to *Rag2*$^{-/-}$ *Tg(Bcl2)* grafts. Data are median +95% confidence interval and at least 6 grafts per time-point are depicted. **(D)** Proliferation was determined in a 2-hour pulse EdU incorporation assay 12, 14 and 16 days after transplant, as indicated. Quantification of EdU-positive thymocytes is depicted for the host derived, *Rag2*$^{-/-}$ DN2 and DN3e thymocytes. (D) Points represent individual grafts and bars correspond to medians. (C,D) Wilcoxon signed-rank test. *p≤0.05, **p≤0.01, ***p≤0.001, **** p<0.0001. Data are representative of a minimum of three independent experiments, except for the data for day 12 after transplant, that was performed once.

Figure 7. DN2b thymocytes proliferate and expand equally well when differentiation takes place in *IL-7rα*$^{+/-}$ thymus grafts, independently of the presence or absence of the *Bcl2* transgene. (A) Schematics of the experimental design. Newborn thymi with the indicated genotypes were transplanted under the kidney capsule of wild type (WT) B6 adult mice. **(B)** Absolute number of host wild type (green bars) and donor derived (*IL-7rα*$^{+/-}$ = black bars, *IL-7rα*$^{+/-}$ *Tg(Bcl2)* = gray bars) thymocytes at different developmental stages during thymus turnover. For each time point, left bar plots represent *IL-7rα*$^{+/-}$ grafts and right bar plots correspond to *IL-7rα*$^{+/-}$ *Tg(Bcl2)* grafts. **(C)** Proliferation was determined in a 2-hour pulse EdU incorporation assay 14 or 16 days after transplant, as indicated. Quantification of EdU-positive thymocytes is depicted for the host derived, wild type DN2 and DN3e thymocytes **(D)** Cell cycle duration of wild type host derived DN2 and DN3e cells that differentiated in *IL-7rα*$^{+/-}$ thymus grafts 14 days after transplant that were either non-transgenic or *Bcl2* transgenic, as indicated. **(E)** Estimates of the proportion of cycling wild type host derived DN2 and DN3e cells that differentiated in *IL-7rα*$^{+/-}$ thymus grafts at 14 days after transplant, either non-transgenic or *Bcl2* transgenic as indicated. (B) Data are median +95% confidence interval and

at least 6 grafts per time-point are depicted. (C, D, E) Points represent individual grafts and bars correspond to medians. Wilcoxon signed-rank test. *p≤0.05, **p≤0.01, ***p≤0.001, **** p<0.0001. (B, C) Data are representative of at least two independent experiments.

Materials and Methods

Mice

C57BL/6J (B6, CD45.2^{+}) were bred and kept at the Instituto Gulbenkian de Ciência (IGC) and frequently renewed with mice purchased from Charles River. *Rag2*$^{-/-}$ (Shinkai et al., 1992) originally purchased from Taconic were also bred and kept at the IGC. B6.SJL-*Ptprc*^{a} Pep3^{b}/BoyJ (CD45.1^{+}) mice, JAX stock #002014, here termed B6/Ly5.1, *IL-7rα*$^{-/-}$ (Peschon et al., 1994), JAX stock #002295, and B6.Cg-Tg(BCL2)25Wehi/J (JAX stock #002320, termed *Tg(Bcl2)*) were purchased from The Jackson Laboratory. All strains used in this work were obtained by crosses between the original strains described here. Thymi for thymus transplants were always harvested from newborn donors in a background F1(B6xB6/Ly5.1), and including the described mutations. All mice were bred and kept in individually ventilated cages in the SPF area of the mouse facility of the Institute. All animal experiments were approved by the Ethics Committee of the IGC – Fundação Calouste Gulbenkian and the Direção Geral de Alimentação e Veterinária (DGAV).

Thymus transplants

Thymus transplants were performed as described previously (Martins et al., 2014; Martins et al., 2012). Briefly, newborn thymus lobes were physically separated and kept in cold PBS until engraftment. Recipient mice aged 6 to 10 weeks were anesthetized with Ketamine (100mg/kg) and Xylazine (16mg/kg) and each recipient received one thymus, grafted under the kidney capsule, with individual lobes at opposite ends.

Cell preparation and flow cytometry

Single-cell suspensions were prepared in PBS/10%FBS. Cell numbers were determined using a hemocytometer, and dead cells excluded by Trypan Blue staining. Cells were blocked for 15 minutes with mouse IgG (112mg/ml, Jackson ImmunoResearch) and stained with an antibody solution

appropriately diluted during 30 minutes. Whenever necessary, after two consecutive washes, the cells were subjected to additional staining steps.

The antibodies and streptavidin, purchased from Biolegend, were as follows: BCL2 Alexa 488 (100), Bcl2 PE (BCL/10C4), BrdU Alexa 647 (3D4), CD3ε bio (145-2C11), CD3ε APC-Cy7 (145-2C11), CD3ε FITC (145-2C11), CD4 PE (GK1.5), CD4 PE-Cy7 (GK1.5), CD4 BV421 (GK1.5), CD4 BV605 (GK1.5), CD8a BV711 (53-6.7), CD8a FITC (YTS169.4), CD8 PerCP-Cy5.5 (53-6.7), CD11b bio (M1/70), CD11c bio (N418), CD19 bio (6D5), CD19 PE-Cy7 (6D5), CD19 BV711 (6D5), CD25 BV421 (PC61), CD25 BV605 (PC61), CD44-PerCP-Cy5.5 (IM7), CD44 BV711 (IM7), CD45.1 APC (A20), CD45.1 BV421 (A20), CD45.1 PE-Cy7 (A20), CD45.2 FITC (104), CD45.2 PerCP-Cy5.5 (104), CD45.2 PE (104), CD45.2 PB (104), CD117 APC (2B8), CD117 APC-Cy7 (2B8), CD127 APC (A7R34), βTCR Alexa 647 (H57-597), βTCR BV711 (H57-597), βTCR FITC (H57-597), βTCR PE (H57-597), γδTCR PE (GL3), γδTCR bio (GL3), Gr-1 bio (RB6-8C5), NK1.1 bio (PK136), NK1.1 A647 (PK136), Ter119 bio (TER-119), streptavidin APC-Cy7, streptavidin BV605 and streptavidin BV785. In the thymus, DN thymocytes were defined as CD4-negative, CD8-negative and Lineage-negative (cocktail composed of CD3, CD11b, CD11c, Ter119, Gr1, NK1.1 and CD19). Dead cell exclusion was done using Sytox Blue (Molecular Probes), Zombie APC-Cy7 or Zombie Pacific Orange (purchased from Biolegend).

Intracellular cell staining was performed by fixing the cells in 4% PFA for 15 minutes at room temperature, followed by intracellular staining using True-Nuclear Transcription Buffer Set (Biolegend) according to manufacturer instructions. Identification of apoptotic cells by Annexin V staining was performed according to manufacturer instructions (Biolegend, cat. 640934). Quantification of proliferation using EdU incorporation was accomplished by IP injection of 0.5mg EdU (Thermo Fisher Scientific cat. E10187). Organs were collected two hours later and the staining procedure was done according to manufacturers' instructions using the Click-it Plus EdU Alexa Fluor 488 Flow Cytometry Assay kit (Molecular Probes). Quantification of cell cycle duration using a

EdU/BrdU double pulse was performed by consecutive i.p. injections of EdU (0.5mg) and BrdU (1mg) two hours apart. Organs were collected and analyzed two hours after the second injection. Following normal staining procedure and fixation in 4% PFA, cells were permeabilized for 15 minutes and incubated for 1 hour at 37ºC in DNase I (300ug/ml PBS, Sigma Aldrich). After washing the staining procedure for EdU was done following manufacturer's instructions, followed by BrdU staining. All acquisitions were performed in a BD LSRFortessa X-20 cell analyzer using BD FACSDiva 8 software and analyses were done using FlowJo.

Immunofluorescence

Thymus grafts were embedded in OCT Compound and snap-frozen in liquid nitrogen. Tissue sections of 8µm were dehydrated in acetone and samples were preserved in a dry environment at -80ºC until staining. Sections were incubated for 30 minutes with DAPI and mIgG in PBS/10%FBS. Following two washes in PBS the samples were stained with CD25 PE (PC61), CD45.2 FITC (104) and Cytokeratin 8 A647 (1E8) overnight at 4ºC. Antibodies were purchased from Biolegend. Stained sections were mounted with mounting medium before acquisition in a Nikon HCS microscope.

Image processing and quantification

Single images and thymus tiles were processed and stitched using Fiji (Schindelin et al., 2012). Donor and host CD25 positive cells were quantified using QuPath (Bankhead et al., 2017). Briefly, thymus sections were subdivided and categorized as cortical or medullary areas and capsule region. Damaged regions were excluded from further analysis. Using a standardized threshold, the number of CD25-positive and CD45.2 positive cells was obtained and their (minimum) distance to the thymus capsule calculated.

Estimation of cell cycle duration

Let p^{+-} be the proportion of $EdU^{+}BrdU^{-}$, p^{++} the proportion of $EdU^{+}BrdU^{+}$, p^{-+} the proportion of $EdU^{-}BrdU^{+}$ and p^{--} the proportion of $EdU^{-}BrdU^{-}$ cells. We consider μ_1 the rate of exit from S phase, μ_2 the rate of entry into S phase, and g_0 the proportion of cells arrested in G_0. The mathematical formalism for cell state transitions between S and G1/G2/M is based on a continuous time 2-state Markov Chain. Assuming a stationary distribution for cell states at the beginning of the experiment, our model describes the proportion of labelled cells after time t (where *t* is the interval between the two labelling pulses) as follows:

$$p^{+-} = \frac{\mu_2}{\mu_1 + \mu_2}(1 - e^{-\mu_1 t})(1 - g_0)$$

$$p^{++} = \frac{\mu_2}{\mu_1 + \mu_2}(e^{-\mu_1 t})(1 - g_0)$$

$$p^{-+} = \frac{\mu_1}{\mu_1 + \mu_2} \times (1 - e^{-\mu_2 t})(1 - g_0)$$

$$p^{--} = \frac{\mu_1}{\mu_1 + \mu_2}(e^{-\mu_2 t})(1 - g_0) + g_0$$

The first term in the equations above corresponds to the stationary proportion of cells in S phase ($\frac{\mu_2}{\mu_1+\mu_2}$) and proportion of cells in G1/G2/M phase ($\frac{\mu_1}{\mu_1+\mu_2}$) at the beginning of experiment, while the other terms describe fluxes and label dynamics. Only cycling cells can acquire at least one of the labels. For example, acquisition of only the first label (EdU, defined as +-) applies to cells that were already in S and cycling, and left S during time t. Similarly, acquisition of only the second label (BrdU, defined as -+) applies to cycling cells that were not in S initially, but entered S during t. A natural assumption in this setup is that cell cycle length exceeds the length of the double pulse.

We fitted the model to the data using nonlinear least-squares approach, which provided approximate solutions for the unknown parameters (μ_1, μ_2, and g_0) from the experimental proportions of labelled

cells. The total duration of the cell cycle (CC) is then given by:

$$CC = \frac{1}{\mu_1} + \frac{1}{\mu_2}$$

Where

$$\frac{1}{\mu_1}$$

Is the mean duration of the S phase, and

$$\frac{1}{\mu_2}$$

is the mean duration of G1/G2/M. The proportion of cycling cells is simply $1\text{-}g_0$.

The model fitting (μ_1, μ_2, g_0) was performed individually for each set of labelled cell proportions (DN2 and DN3e) across different conditions. The estimates were gathered by graft genotype and by day, and subsequently compared.

Statistical analyses

Statistical analyzes were performed using R software unless stated otherwise. Significance values were computed using Wilcoxon rank-signed test. If data followed a normal distribution according to the Shapiro-Wilk test, unpaired two-tailed Student's *t*-test was used.

REFERENCES

Akashi, K., Kondo, M., von Freeden-Jeffry, U., Murray, R., and Weissman, I.L. (1997). Bcl-2 rescues T lymphopoiesis in interleukin-7 receptor-deficient mice. Cell *89*, 1033-1041.

Akinduro, O., Weber, T.S., Ang, H., Haltalli, M.L.R., Ruivo, N., Duarte, D., Rashidi, N.M., Hawkins, E.D., Duffy, K.R., and Lo Celso, C. (2018). Proliferation dynamics of acute myeloid leukaemia and haematopoietic progenitors competing for bone marrow space. Nat Commun *9*, 519.

Amoyel, M., and Bach, E.A. (2014). Cell competition: how to eliminate your neighbours. Development *141*, 988-1000.

Baker, N.E. (2017). Mechanisms of cell competition emerging from Drosophila studies. Curr Opin Cell Biol *48*, 40-46.

Ballesteros-Arias, L., Silva, J.G., Paiva, R.A., Carbonetto, B., Faisca, P., and Martins, V.C. (2019). T Cell Acute Lymphoblastic Leukemia as a Consequence of Thymus Autonomy. J Immunol *202*, 1137-1144.

Bankhead, P., Loughrey, M.B., Fernandez, J.A., Dombrowski, Y., McArt, D.G., Dunne, P.D., McQuaid, S., Gray, R.T., Murray, L.J., Coleman, H.G., *et al.* (2017). QuPath: Open source software for digital pathology image analysis. Sci Rep *7*, 16878.

Barata, J.T., Durum, S.K., and Seddon, B. (2019). Flip the coin: IL-7 and IL-7R in health and disease. Nat Immunol *20*, 1584-1593.

Berzins, S.P., Boyd, R.L., and Miller, J.F. (1998). The role of the thymus and recent thymic migrants in the maintenance of the adult peripheral lymphocyte pool. J Exp Med *187*, 1839-1848.

Boehm, T. (2012). Self-renewal of thymocytes in the absence of competitive precursor replenishment. J Exp Med *209*, 1397-1400.

Bondar, T., and Medzhitov, R. (2010). p53-mediated hematopoietic stem and progenitor cell competition. Cell stem cell *6*, 309-322.

Cao, X., Shores, E.W., Hu-Li, J., Anver, M.R., Kelsall, B.L., Russell, S.M., Drago, J., Noguchi, M., Grinberg, A., and Bloom, E.T. (1995). Defective lymphoid development in mice lacking expression of the common cytokine receptor gamma chain. Immunity *2*, 223-238.

Claveria, C., and Torres, M. (2016). Cell Competition: Mechanisms and Physiological Roles. Annu Rev Cell Dev Biol *32*, 411-439.

Di Gregorio, A., Bowling, S., and Rodriguez, T.A. (2016). Cell Competition and Its Role in the Regulation of Cell Fitness from Development to Cancer. Dev Cell *38*, 621-634.

DiSanto, J.P., Muller, W., Guy-Grand, D., Fischer, A., and Rajewsky, K. (1995). Lymphoid development in mice with a targeted deletion of the interleukin 2 receptor gamma chain. Proc Natl Acad Sci U S A *92*, 377-381.

Eichenlaub, T., Cohen, S.M., and Herranz, H. (2016). Cell Competition Drives the Formation of Metastatic Tumors in a Drosophila Model of Epithelial Tumor Formation. Curr Biol *26*, 419-427.

Frey, J.R., Ernst, B., Surh, C.D., and Sprent, J. (1992). Thymus-grafted SCID mice show transient thymopoiesis and limited depletion of V beta 11+ T cells. J Exp Med *175*, 1067-1071.

Ginn, S.L., Hallwirth, C.V., Liao, S.H., Teber, E.T., Arthur, J.W., Wu, J., Lee, H.C., Tay, S.S., Hu, M., Reddel, R.R.*, et al.* (2017). Limiting Thymic Precursor Supply Increases the Risk of Lymphoid Malignancy in Murine X-Linked Severe Combined Immunodeficiency. Mol Ther Nucleic Acids *6*, 1-14.

Johnston, L.A. (2009). Competitive interactions between cells: death, growth, and geography. Science *324*, 1679-1682.

Katsumata, M., Siegel, R.M., Louie, D.C., Miyashita, T., Tsujimoto, Y., Nowell, P.C., Greene, M.I., and Reed, J.C. (1992). Differential effects of Bcl-2 on T and B cells in transgenic mice. Proc Natl Acad Sci U S A *89*, 11376-11380.

Kon, S., Ishibashi, K., Katoh, H., Kitamoto, S., Shirai, T., Tanaka, S., Kajita, M., Ishikawa, S., Yamauchi, H., Yako, Y.*, et al.* (2017). Cell competition with normal epithelial cells promotes apical extrusion of transformed cells through metabolic changes. Nature cell biology *19*, 530-541.

Kondo, M., Akashi, K., Domen, J., Sugamura, K., and Weissman, I.L. (1997). Bcl-2 rescues T lymphopoiesis, but not B or NK cell development, in common gamma chain-deficient mice. Immunity *7*, 155-162.

Lind, E.F., Prockop, S.E., Porritt, H.E., and Petrie, H.T. (2001). Mapping precursor movement through the postnatal thymus reveals specific microenvironments supporting defined stages of early lymphoid development. J Exp Med *194*, 127-134.

Love, P.E., and Bhandoola, A. (2011). Signal integration and crosstalk during thymocyte migration and emigration. Nat Rev Immunol *11*, 469-477.

Madan, E., Pelham, C.J., Nagane, M., Parker, T.M., Canas-Marques, R., Fazio, K., Shaik, K., Yuan, Y., Henriques, V., Galzerano, A.*, et al.* (2019). Flower isoforms promote competitive growth in cancer. Nature *572*, 260-264.

Martin, C.E., Spasova, D.S., Frimpong-Boateng, K., Kim, H.O., Lee, M., Kim, K.S., and Surh, C.D. (2017). Interleukin-7 Availability Is Maintained by a Hematopoietic Cytokine Sink Comprising Innate Lymphoid Cells and T Cells. Immunity *47*, 171-182 e174.

Martins, V.C., Busch, K., Juraeva, D., Blum, C., Ludwig, C., Rasche, V., Lasitschka, F., Mastitsky, S.E., Brors, B., Hielscher, T., *et al.* (2014). Cell competition is a tumour suppressor mechanism in the thymus. Nature *509*, 465-470.

Martins, V.C., Ruggiero, E., Schlenner, S.M., Madan, V., Schmidt, M., Fink, P.J., von Kalle, C., and Rodewald, H.R. (2012). Thymus-autonomous T cell development in the absence of progenitor import. J Exp Med *209*, 1409-1417.

Maruyama, T., and Fujita, Y. (2017). Cell competition in mammals - novel homeostatic machinery for embryonic development and cancer prevention. Curr Opin Cell Biol *48*, 106-112.

Mazel, S., Burtrum, D., and Petrie, H.T. (1996). Regulation of cell division cycle progression by bcl-2 expression: a potential mechanism for inhibition of programmed cell death. J Exp Med *183*, 2219-2226.

Morata, G., and Ballesteros-Arias, L. (2014). Developmental Biology. Death to the losers. Science *346*, 1181-1182.

Morata, G., and Ripoll, P. (1975). Minutes: mutants of drosophila autonomously affecting cell division rate. Dev Biol *42*, 211-221.

Moreno, E. (2008). Is cell competition relevant to cancer? Nature reviews. Cancer *8*, 141-147.

O'Reilly, L.A., Harris, A.W., and Strasser, A. (1997). bcl-2 transgene expression promotes survival and reduces proliferation of CD3-CD4-CD8- T cell progenitors. Int Immunol *9*, 1291-1301.

Paiva, R.A., Ramos, C.V., and Martins, V.C. (2018). Thymus autonomy as a prelude to leukemia. FEBS J *285*, 4565-4574.

Peaudecerf, L., Lemos, S., Galgano, A., Krenn, G., Vasseur, F., Di Santo, J.P., Ezine, S., and Rocha, B. (2012). Thymocytes may persist and differentiate without any input from bone marrow progenitors. J Exp Med *209*, 1401-1408.

Peschon, J.J., Morrissey, P.J., Grabstein, K.H., Ramsdell, F.J., Maraskovsky, E., Gliniak, B.C., Park, L.S., Ziegler, S.F., Williams, D.E., Ware, C.B., *et al.* (1994). Early lymphocyte expansion is severely impaired in interleukin 7 receptor-deficient mice. J Exp Med *180*, 1955-1960.

Petrie, H.T., and Zuniga-Pflucker, J.C. (2007). Zoned out: functional mapping of stromal signaling microenvironments in the thymus. Annu Rev Immunol *25*, 649-679.

Porritt, H.E., Gordon, K., and Petrie, H.T. (2003). Kinetics of steady-state differentiation and mapping of intrathymic-signaling environments by stem cell transplantation in nonirradiated mice. J Exp Med *198*, 957-962.

Prockop, S.E., and Petrie, H.T. (2004). Regulation of thymus size by competition for stromal niches among early T cell progenitors. J Immunol *173*, 1604-1611.

Rothenberg, E.V. (2019). Programming for T-lymphocyte fates: modularity and mechanisms. Genes Dev *33*, 1117-1135.

Schindelin, J., Arganda-Carreras, I., Frise, E., Kaynig, V., Longair, M., Pietzsch, T., Preibisch, S., Rueden, C., Saalfeld, S., Schmid, B.*, et al.* (2012). Fiji: an open-source platform for biological-image analysis. Nat Methods *9*, 676-682.

Schiroli, G., Ferrari, S., Conway, A., Jacob, A., Capo, V., Albano, L., Plati, T., Castiello, M.C., Sanvito, F., Gennery, A.R.*, et al.* (2017). Preclinical modeling highlights the therapeutic potential of hematopoietic stem cell gene editing for correction of SCID-X1. Sci Transl Med *9*, eaan0820.

Shinkai, Y., Rathbun, G., Lam, K.P., Oltz, E.M., Stewart, V., Mendelsohn, M., Charron, J., Datta, M., Young, F., Stall, A.M., and Alt, F.W. (1992). RAG-2-deficient mice lack mature lymphocytes owing to inability to initiate V(D)J rearrangement. Cell *68*, 855-867.

Strasser, A., Harris, A.W., and Cory, S. (1991). bcl-2 transgene inhibits T cell death and perturbs thymic self-censorship. Cell *67*, 889-899.

Suijkerbuijk, S.J., Kolahgar, G., Kucinski, I., and Piddini, E. (2016). Cell Competition Drives the Growth of Intestinal Adenomas in Drosophila. Curr Biol *26*, 428-438.

Surh, C.D., and Sprent, J. (2008). Homeostasis of naive and memory T cells. Immunity *29*, 848-862.

Takahama, Y., Ohigashi, I., Baik, S., and Anderson, G. (2017). Generation of diversity in thymic epithelial cells. Nat Rev Immunol *17*, 295-305.

Takeda, S., Rodewald, H.R., Arakawa, H., Bluethmann, H., and Shimizu, T. (1996). MHC class II molecules are not required for survival of newly generated CD4+ T cells, but affect their long-term life span. Immunity *5*, 217-228.

Tan, J.B., Visan, I., Yuan, J.S., and Guidos, C.J. (2005). Requirement for Notch1 signals at sequential early stages of intrathymic T cell development. Nat Immunol *6*, 671-679. Epub 2005 Jun 2012.

Visan, I., Tan, J.B., Yuan, J.S., Harper, J.A., Koch, U., and Guidos, C.J. (2006). Regulation of T lymphopoiesis by Notch1 and Lunatic fringe-mediated competition for intrathymic niches. Nat Immunol *7*, 634-643.

von Freeden-Jeffry, U., Vieira, P., Lucian, L.A., McNeil, T., Burdach, S.E., and Murray, R. (1995). Lymphopenia in interleukin (IL)-7 gene-deleted mice identifies IL-7 as a nonredundant cytokine. J Exp Med *181*, 1519-1526.

Yui, M.A., and Rothenberg, E.V. (2014). Developmental gene networks: a triathlon on the course to T cell identity. Nat Rev Immunol *14*, 529-545.

Figure 1

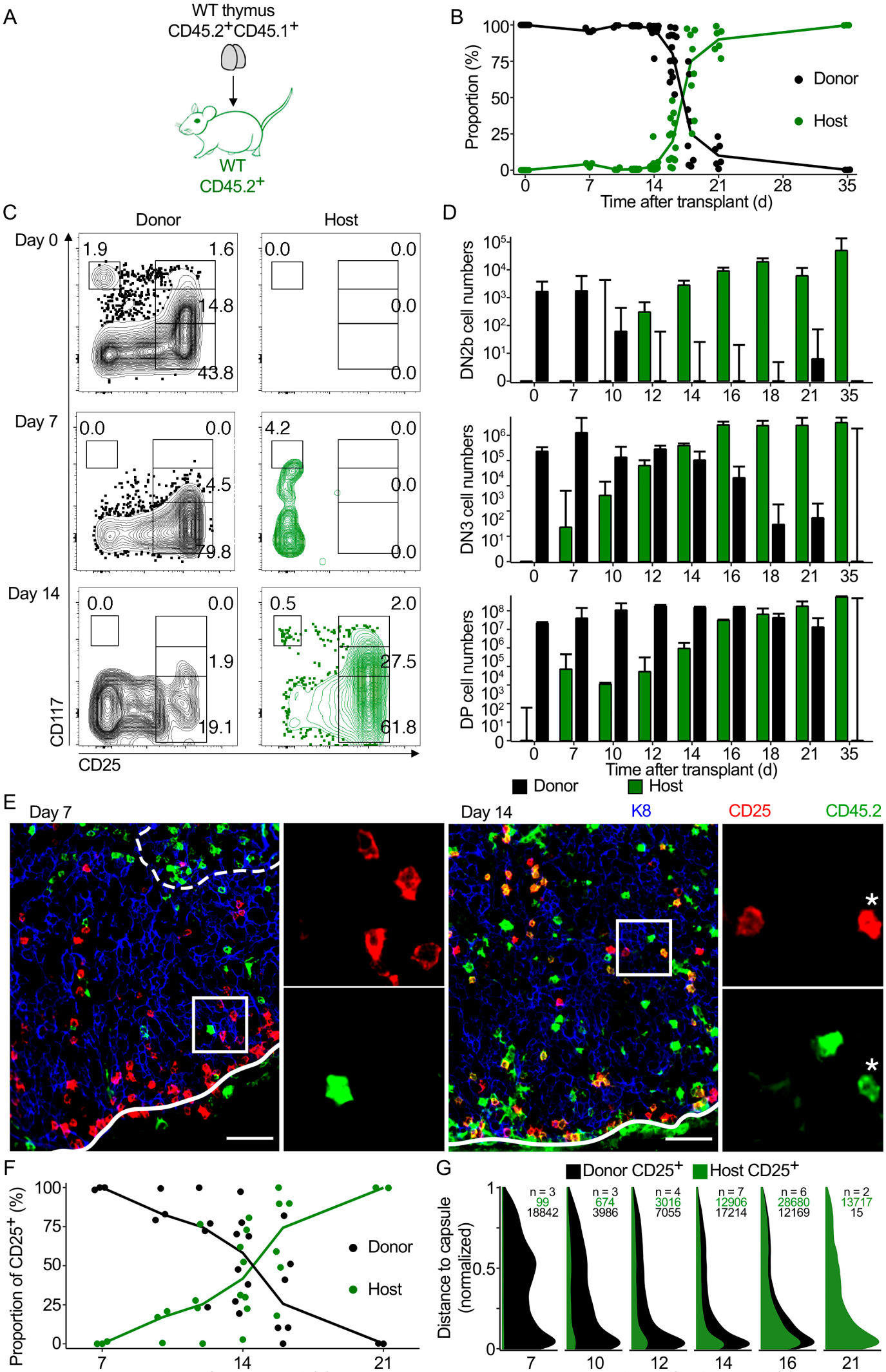

Figure 2

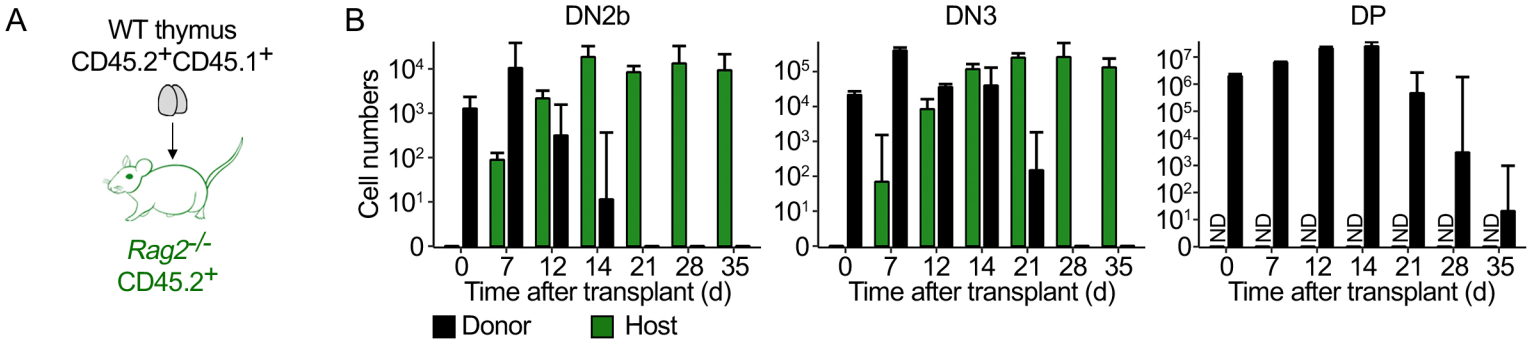

Figure 3

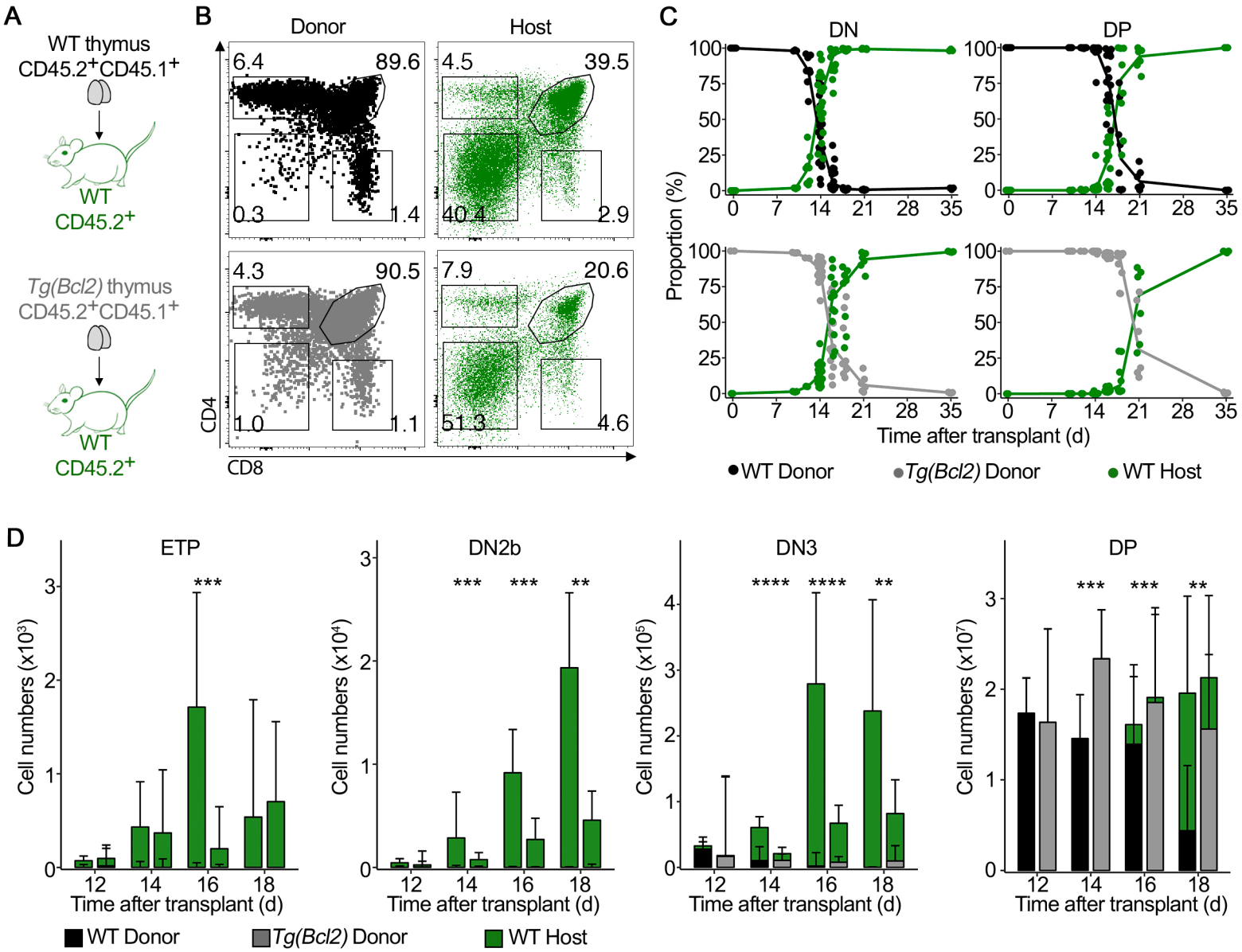

Figure 4

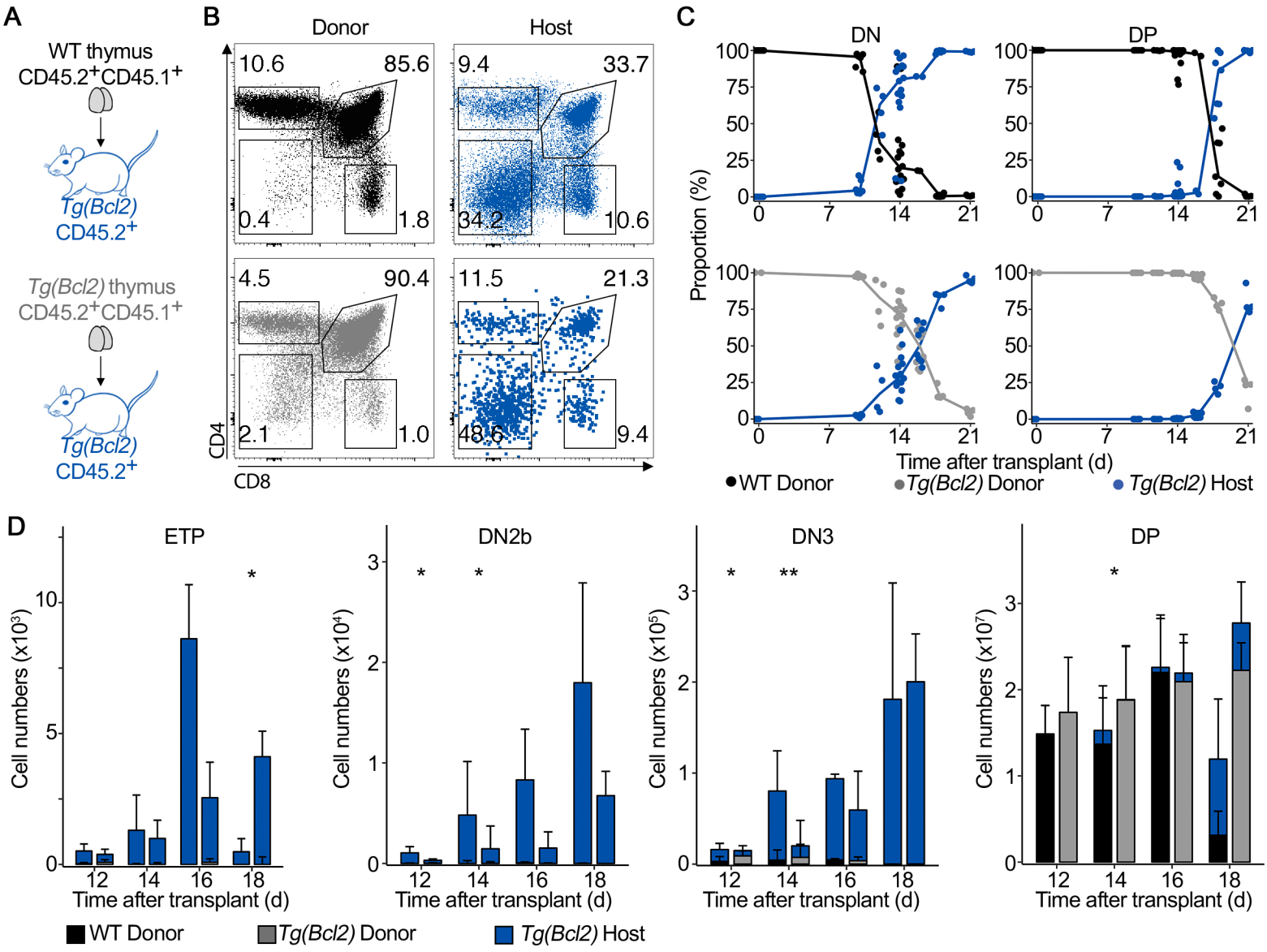

Figure 5

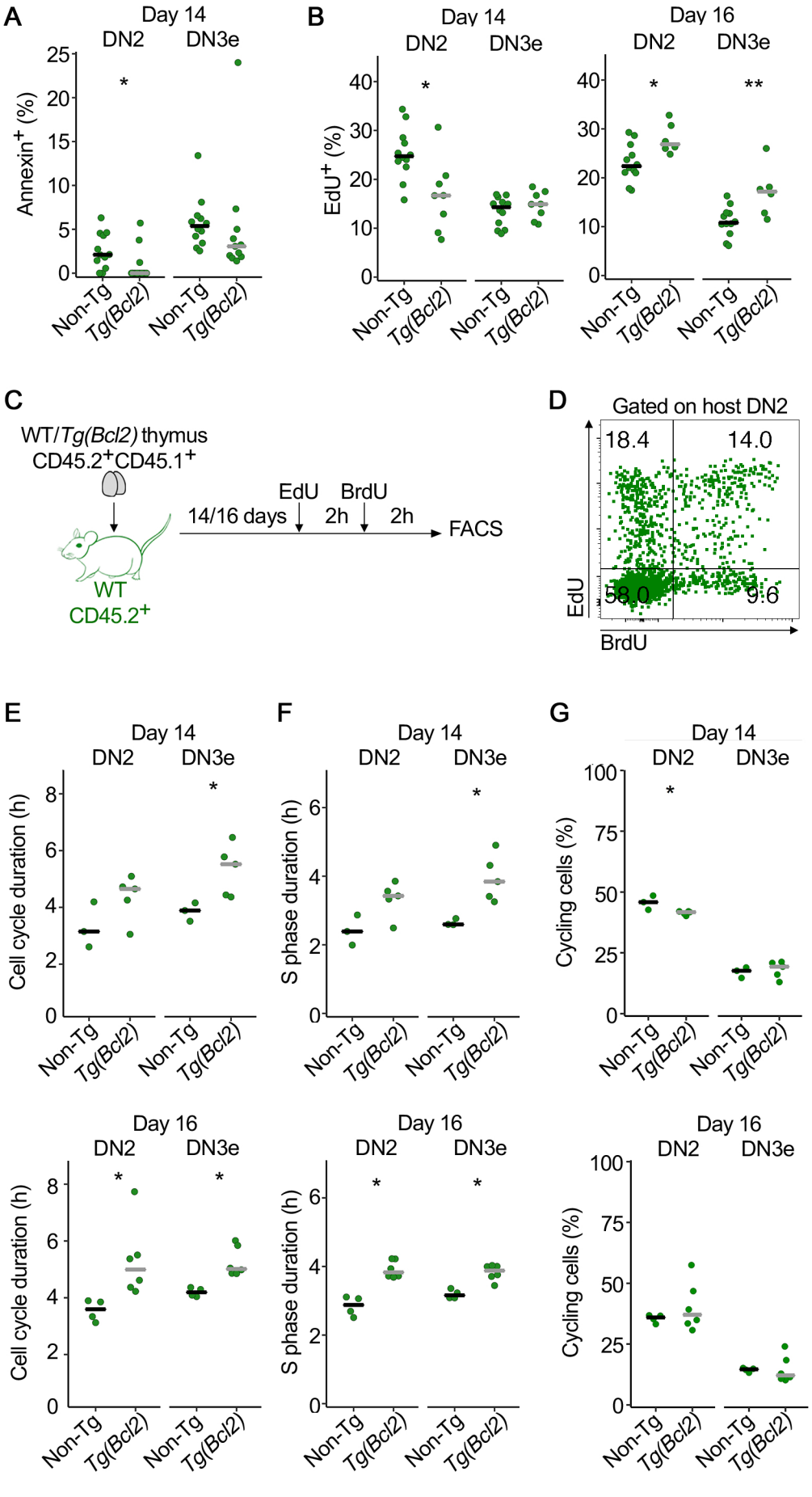

Figure 6

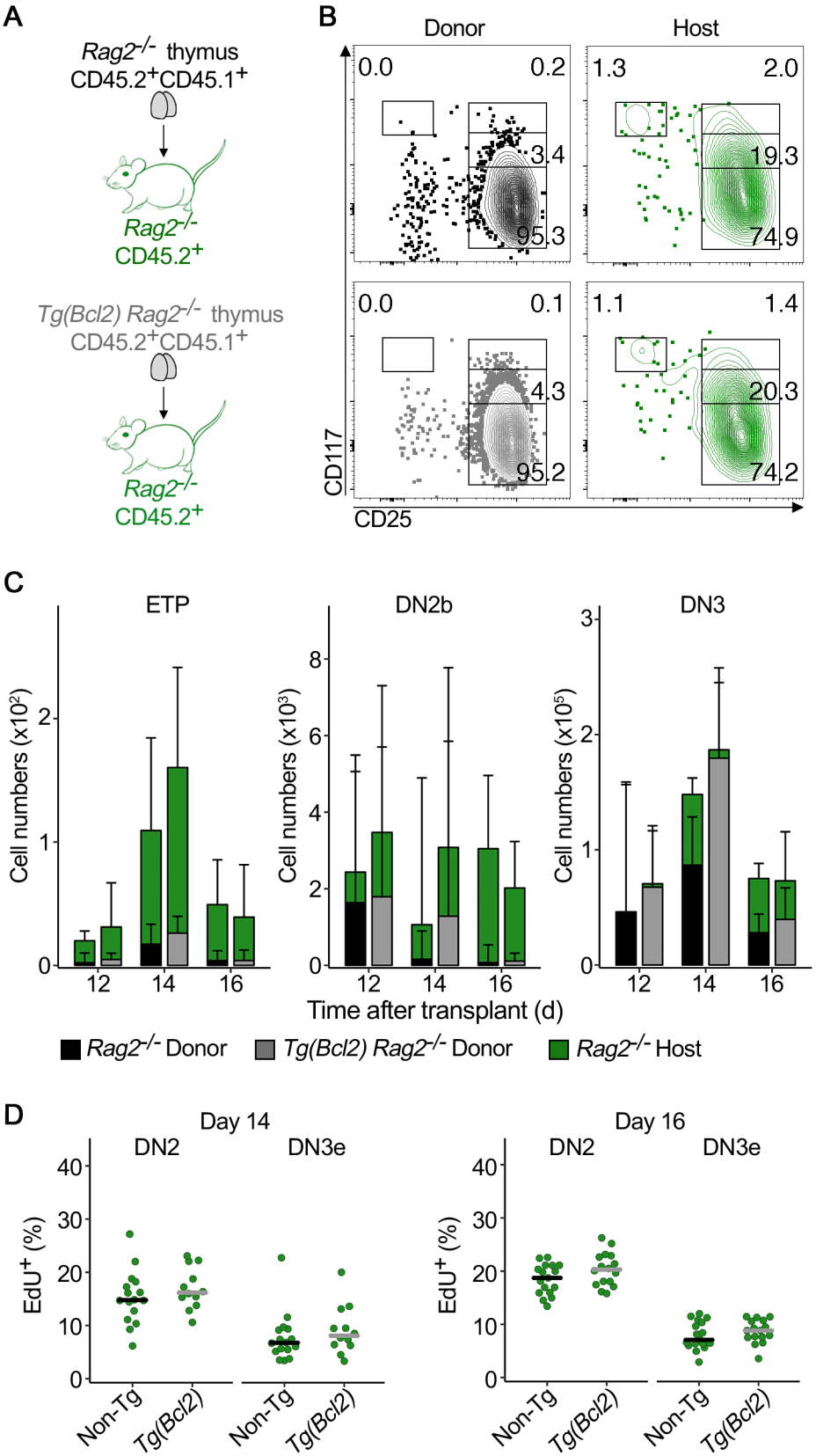

Figure 7